Significant improvement of sperm motility parameters through surface modification with Nano Diamond particles

Ali lesani[1,*], Somaieh Kazemnejad [2], Hengameh Mousavi[3], Iman Ramazani Sarbandi[1], Mahdi Moghimi Zand[1]

[1] BioMEMS and LoC lab, Faculty of Mechanical Engineering, University of Tehran, Iran
[2] Reproductive Biotechnology Research Center, Avicenna Research Institute, ACECR, Tehran, Iran
[3] Faculty of Physics, Nano Science and Technology, Damghan University, Damghan, Iran

* Corresponding Author:
Ali.lesani@ut.ac.ir (Ali Lesani)

Abstract

The employment of Nanotechnology as a valuable tool could be beneficial to patients and also offer new alternatives for Assisted Reproductive Technology (ART). Surface modification by nanoparticles leads to the alteration of surface characteristics (e.g. roughness, elasticity, and surface charge). These alterations affect sperm behavior especially its motility since sperms exhibit wall following behavior and surface accumulation. Moreover, surface modification is an attempt towards mimicking the complex in vivo environment of the female tract (highly folded and ciliated) with continually changing surface topology and also its functions. In this paper, we present the results of investigating the interactions between sperm cells and surface modified substrates using Nano diamond particles. A combinational and low-cost method was used for modification. The results show that the sperm motility parameters are significantly improved from 5 to 85%. Also, the results indicate that in optimized surface modification condition, the sperms swim faster and straighter and the surface facilitates the swimming due to the inherent characteristics of ND particles.
Taken together, the replacement of normal with modified surfaces in fertility-aid microfluidic devices can enhance their efficiency and further improve their outcomes.

Keywords: Sperm motility, Nano Diamond, Surface modification, Microfluidics, Nanotechnology

1. Introduction

Motility of the sperms plays a key role in traversing the long path of the female tract and subsequently in their success of fertilization. The effects of different parameters on motility such as the flow [1-3], chemical environment [4-6], and temperature [7-9] have been studied so far. Among all, confinement and contact surface are known to be effective on sperm motility but their details remain unexplored.

When it comes to the surface, the wall following behavior and surface accumulation of sperms are highlighted. While near the wall, the hydrodynamic flow field loses its symmetry and results in surface accumulation [10]. Moreover, the interaction between the flagellar wave of human sperm and the surface, guides the swimming trajectory towards it being dependent on sperm distance from the surface and its orientation [11, 12]. The surface can also influence the group behavior of the sperms leading to the synchronized tail beatings and increasing the swimming velocity [13].

Apart from hydrodynamic parameters that affect surface accumulation, geometrical constraints of the surface play the same role [14]. In this essence, the existence of nonplanar surfaces and surface roughness significantly changes sperm motion since the majority of sperms swim near the wall. This following behavior is observed at curvatures more than 150 micrometers otherwise rather sharp curvatures result in the repulsion of the sperms from the surface [15]. Many studies had focused on sperm motion in contact with flat surfaces, but in vivo geometries are more complex (highly folded and ciliated and continually changing) and relevant swimming behavior needs to be further addressed. This calls for bio-inspired micro/nanotechnologies to enter the arena and fully unveil the effects of geometrical complexity on sperm motion especially through surface modification.

Surface modification leads to the alteration of surface characteristics such as roughness [16, 17], mechanical properties [18, 19], hydrophilicity [20, 21], biocompatibility [22-24], and surface charge [25]. It can be achieved through different physical and chemical methods making the surface exhibit enhanced and even new characteristics with or without the use of external micro/nanoparticles. Expensive and substrate-specific methods exist in the former category as chemical vapor deposition (CVD) which limits the extensive usage of particles and their possible benefits. While, combinational modification methods could be helpful for their relatively lower cost and modification capability of various substrates. Finally, the combination of surface modification and microscopy provides an opportunity for understanding the interaction between modified surfaces and sperm motility.

Here, we used the combination of chemical etching and spin coating methods to modify the surface of widely-used microscope glass substrates with Nanodiamond (ND) particles for their unique biocompatibility and inherent potentials. The objective of the present study is to investigate the interaction of sperm cells with ND modified surfaces under the geometrical change in surface topology along with the ND coating itself.

2. Materials and Methods

2.1. Surface modification with ND particles

2.1.1. Preparation of ND suspension

Commercially available Nanodiamond powder (Shenzhen Jingangyuan New Material Development Co., Ltd., China) with the purity of 95% percent and average size of 50 nm was purchased. The ND

particles were then added to acetone (1:10 ratio). The mixture was sonicated in 50 cycles for 20 minutes with an ultrasonic homogenizer sonotrode supplied by 90 W power (FAPAN, Iran). TEM was used to characterize the morphology and particle size of the dispersed particles in the solution. Finally, three different concentrations of the suspension as 1, 0.6, and 0.4 g/l v/v were prepared.

2.1.2. Substrate etching

The etching process of the microscope glass substrate included 6 steps. The procedure started with the immersion of the surfaces in a 50% v/v solution of H_2SO_4 (95%) and H_2O_2 (30%) for 3 days. The surfaces were rinsed after 3 days with distilled water until the stabilization of the solution pH. The surfaces were immersed in a solution of HNO_3 (5 mol/l) for another 3 days. The rinsing was repeated on the fourth day. The procedure continued by the immersion of substrates in NaOH solution (4 mol/l) for 3 minutes with simultaneous heating at 55°C on a hot plate. The excess NaOH was then removed from the substrates with distilled water and they were again immersed in HNO_3 solution (5 mol/l) for 3 days. Having rinsed the surfaces on day 4 with distilled water, they were transferred to a furnace and dried at 60°C for 8 hours. The procedure was adopted from [26].

2.1.3. Spin coating

The etched microscope glass substrates were first divided into 2.5×2.5 cm squares. Prepared ND suspensions were spin coated on the etched microscope glass substrates in 30 seconds using a custom-built spin coater (Nanostructured Materials & Composites (NMC) lab, Faculty of material engineering, university of Tehran) with fixed droplet volume of 50 µl and varying rotational speed (2000 and 3000 rpm), and ND concentration (1, 0.6, and 0.4% v/v). Afterwards, the effect of droplet volume on the optimized surface was also investigated (50 and 100 µl). To ensure the repeatability of the results, the spin coating in each case was done on three different substrates.

2.1.4. Furnace heating

The marked spin coated substrates were then transferred to an electric furnace (Fan Azma Gostar, Iran) and heated for 3 hours at 100°C and packed for testing.

2.2. Sperm sample preparation

Three discarded fresh routine semen analysis samples were consecutively collected from the Avicenna Infertility Clinic (Tehran, Iran). Collected semen specimens were liquefied and prepared by standard swim-up technique. In brief, 1 ml of whole semen was gently mixed with 1 ml of Ham's F10 medium (Sigma, USA), supplemented with human serum albumin (3%) (Sigma, USA) and centrifuged (330×g for 10 min). The supernatant was removed and 2 ml of "Ham's F-10" medium was added to the pellet. In this study, 3 µl of washed semen remnant was used for substrate testing.

2.3. Sperm Imaging

The witness and spin coated substrates were incubated for 10 min at 37°C prior to imaging. A 3 μl droplet of the same sperm sample was applied to the center of the glass substrates followed by adding a coverslip. An optical microscope (Olympus CX21, China) was used for imaging with magnification of 40x. A 2MP Microscope Imager Digital USB Camera (Eyescope, NXM-EPA200) was mounted on the microscope eye and used to capture image sequences with 16 Hz frame rate. The imaging of each substrate was performed for 1 min.

2.4. Sperm motion analysis

Quantitative motion analysis was performed using freely available ImageJ software. Manual tracking was utilized to calculate sperm position in the XY plane. Thereafter, a custom-written Matlab code [27] was used to derive motility parameters according to computer-aided sperm analysis (CASA) standards along with swimming trajectories. The motility parameters included Curvilinear velocity (VCL), Average path velocity (VAP), Straight line velocity (VSL), Linearity (LIN), Mean curvature (MCR), and The amplitude of lateral head displacement (ALH) according to [27]. 12 sperms were tracked and followed for at least 40 frames in each case. The values were averaged over each trajectory and the trajectory-wise mean over the number of trajectories was considered as the final value.

2.5. Atomic Force Microscopy (AFM)

AFM technique was used to visualize and compare the topography of witness and spin coated surfaces. The AFM z (x, y) maps were used to estimate some texture parameters allowing for surface roughness characterization, respectively $\bar{R}$ and R_{rms} were defined as:

$$\bar{R} = \frac{1}{x_{max}} \int_0^{x_{max}} |z(x)| dx \qquad (1)$$

$$R_{rms} = \sqrt{\frac{1}{x_{max}} \int_0^{x_{max}} z^2 dx} \qquad (2)$$

where z (x, y) is the height of the surface element at point (x, y) and x_{max} is the maximum value of the lateral displacement x during the measurements, for a given value of y. Surface morphology and roughness of each surface were measured with a Nanosurf easyScan2 (Nanosurf, Liestal, Switzerland) atomic force microscope (AFM) in tapping mode in air. Silicon cantilever tip (Budget Sensors, Innovative Solutions Bulgaria Ltd., Sofia, Bulgaria) with resonant frequency of 190 kHz and with 48 N/m force constant and tip radii lower than 10 nm were used for measurements.

EasyScan 2 software (Nanosurf, Liestal, Switzerland) was used to analyze the data and estimate the root mean squared (RMS) roughness. The AFM images dimensions were 100 × 100 μm. An image

consists of multiple scans displaced laterally from each other in the y direction. Low-pass filtering was performed to remove the statistical noise without loss of information. AFM measurements were repeated on different sites of the sample, keeping the same conditions of room temperature and ambient atmosphere.

2.6. X-Ray Diffraction Analysis

X-ray Diffraction (XRD) analysis was performed on modified substrates by a diffractometer (STOE, STADI MP, Germany) with a Cu X-ray tube throughout the process. Diffraction angles (2θ) in the range of 10 to 100 were analyzed at 0.04 $^{\circ}/s$ searching for diamond peaks. The XRD spectra was background corrected through polynomial subtraction, and noise was reduced with a Savitsky-Golay filter and the graphs were regenerated using Origin software (Origin (Pro), 2018, OriginLab Corporation).

2.7. Contact Angle Measurement

Contact angle measurements (sessile drop technique) was also carried out on the witness and the best modified surface with bi-distilled water. The static sessile drop contact angle between the surface and the tangent line starting from the three-phase point was measured using a contact angle goniometer using an optical subsystem to capture the profile of a pure liquid on a solid surface (Jikan CAG-10, Iran). Furthermore, the contact angle magnitude was measured using the complemented software designed for drop shape analysis.
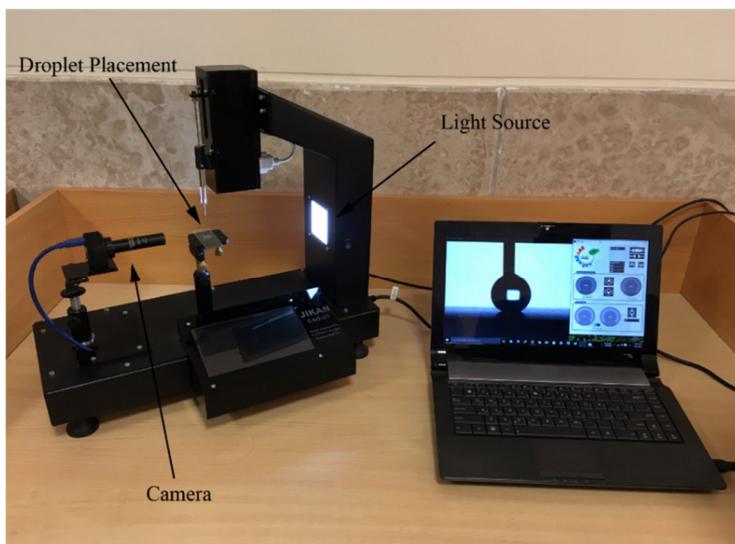

Fig. 1 Contact Angle Measurement Setup composed of Goniometer and analysis software.

3. Results and Discussion

The ND particles were successfully spin coated and stabilized on the glass substrates. Fig. 2a shows the TEM image that characterizes the dispersed nanoparticles in terms of size showing a cluster of the particles with approximate size of 50 nm. Fig. 2b shows the XRD image taken from one of the modified surfaces spin coated with 1 g/l concentration of ND particles. Diamond peaks were detectable in the modified spectra (green line) with different 2θ positions matching the first peak of the base spectra (blue line) at 44.12° corresponding (111) lattice plane which proves the existence of the ND particles on the surface. However, the peak intensity is not high (one order of magnitude lower than pure diamond) due to the low concentration of ND particles in the prepared suspension.
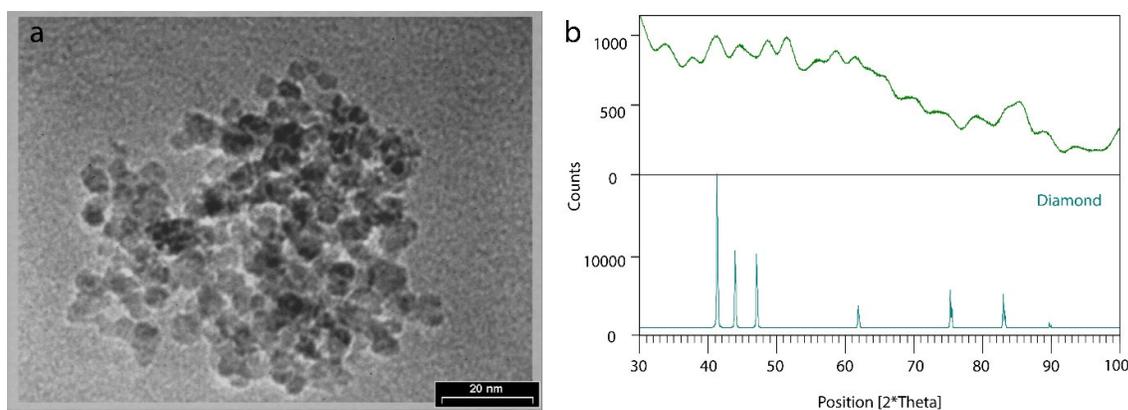

Fig. 2 (a) TEM image of the dispersed ND particles in the prepared suspension. The cluster of diamond crystals is 50 nm in size. (b) Modified XRD spectra (green line) for the spin coated substrate with 1 g/l concentration of ND particles in the prepared suspension. Matching of the first diamond peak at 44.12° corresponding (111) lattice with the base spectra (blue line) plane proves the existence of the ND particles on the surface.

3.1. Sperm motion analysis on ND-coated surfaces

Figure 3 details the motility parameters of human sperm on different glass substrates modified by combinations of ND concentration (1, 0.6, and 0.4 g/l) and spin coating rotational speed (2000 and 3000 rpm) compared to the witness surface (control). As compared to the witness surface under similar conditions, modified surfaces exhibited VSL, VCL and VAP increase between 5– 51%, 3– 53% and 1–37% (min—max), respectively (Fig. 3a–c). The maximum enhancement occurs in VSL, VCL, and VAP by 51, 53, and 37% respectively for the case with 1 g/l ND concentration and 2000 rpm rotational speed (2000-c1).
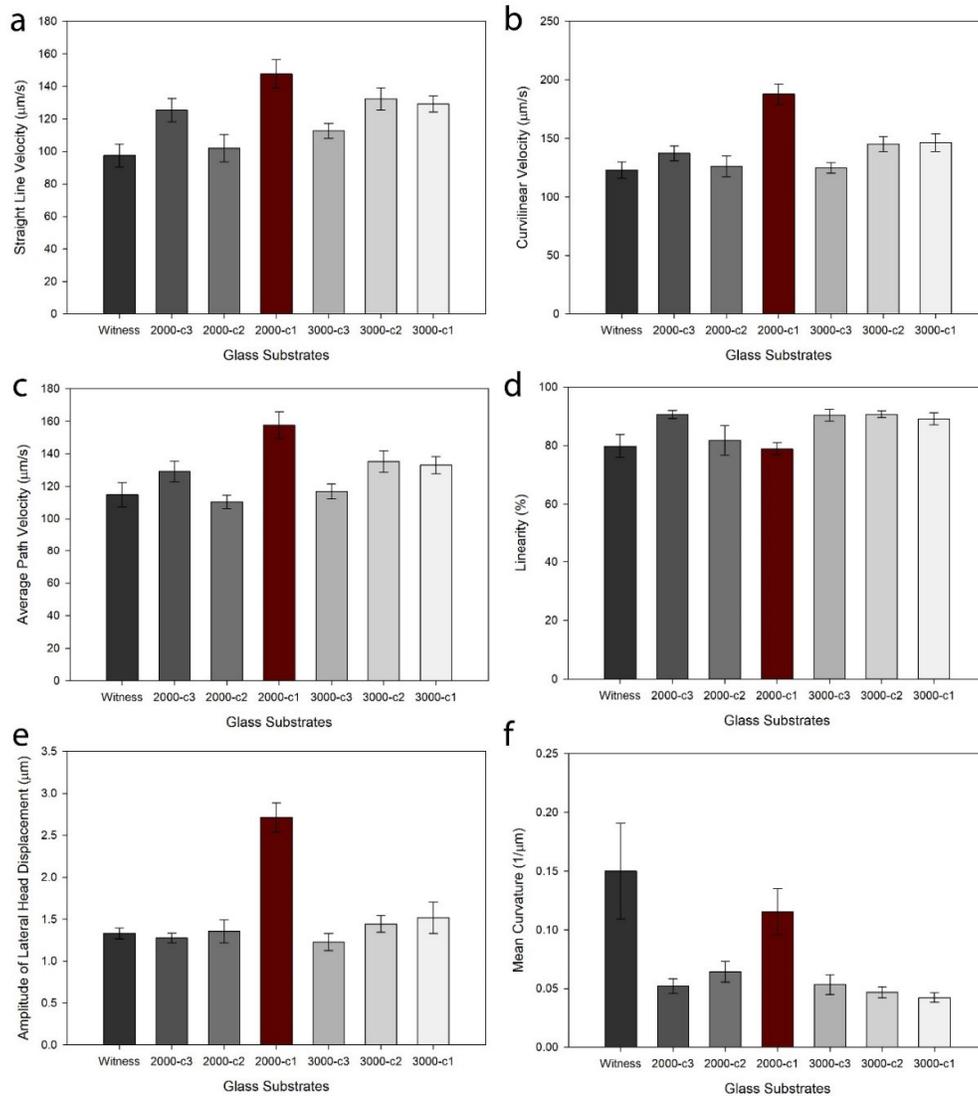
Fig. 3 Human sperm motility parameters on different glass substrates modified by combinations of ND concentration (1, 0.6, and 0.4 g/l) and spin coating rotational speed (2000 and 3000 rpm) compared to the witness surface (control). (a) straight line velocity (VSL), (b) curvilinear velocity (VCL), (c) average path velocity (VAP), (d) linearity (LIN), (e) amplitude of lateral head displacement (ALH), (f) and mean curvature (MCR) for human sperm swimming on the substrates. Values are reported as mean±s.d. Apart from the witness, the modified substrates are named by a hyphenated statement as '*spin coating rotational speed*'- '*ND concentration(c_i)*' in which c1 stands for 1 g/l, c2 for 0.6, and c3 for 0.4 g/l concentration.

Linearity (LIN) was higher in most substrates by 9% in average. Among the substrates, only the 2000-c1 case that acquired the highest rank in velocity enhancement, did not show significant increase being almost equal to the witness (Fig 3(d)). The increase in linearity implies that sperm follow straighter trajectories on the modified surfaces. The amplitude of lateral head displacement (ALH) increased significantly, from 1.33 μm for the witness to 2.71 μm for the 2000-c1 case (P<0.001 with a t-test) and 19% in average (Fig 3(e)). Regarding the MCR of the instantaneous sperm trajectory, it was decreased considerably for all the modified surfaces ranging from 23% to 71% as compared with the witness (Fig. 3(f)), indicating an increase in symmetry of the flagellar wave. This significant

reduction in oscillations may contribute to the increased velocity and LIN experienced on ND-modified surfaces.

Results indicate that the sperm motility is generally enhanced on ND-modified substrates with 1 g/l and 2000 rpm case exhibiting the highest enhancements as compared to other cases. This can be explained with the higher concentration of ND particles used for spin coating. Moreover, compared to 3000 rpm, it shows that the lower rotational speed improves the distribution of ND particles on the surface rather than splashing of the applied droplet.

To further investigate the effect of droplet volume, six substrates were modified based on 2000-c1 case, three of which spin coated with 50µl droplet volume and the remaining with 100µl. Table 1 summarizes the key motility parameters for human sperm swimming on both substrates.

Table 1 Comparative swimming characteristics of sperms on 2000-c1 modified surface by varying droplet volume of 50µl and 100µl.

Parameters	50µl droplet volume (n=36)	100µl droplet volume (n=36)
VSL (µm/s)	147.69±8.66	180.12±5.01
VCL (µm/s)	187.85±8.68	215.39±5.13
VAP (µm/s)	157.53±8.19	184.01±4.75
LIN (%)	78.89±2.03	82.82±2.16
WOB (%)	84.12±1.99	85.13±1.86
MCR (1/µm)	0.12±0.02	0.07±0.004
ALH (µm)	2.71±0.17	2.78±0.07
BCF (Hz)	25.42±1.87	29.55±2.29

Comparing the motility parameters shows that as the droplet volume increases, the better distribution of ND particles occurs on the surface leading to significant enhancement in VSL, VCL, and VAP. It also shows 5% improvement in LIN, 6% increase in BCF and the reduction of mean curvature by 60%. However, the WOB and ALH were almost constant for both substrates being insensitive to droplet volume.

Taken together, these observations indicate that sperm swim faster with improved linear progressive motility on ND-modified surface as compared with witness. When considering assisted reproduction, progressive motility of sperm is essential to ensure the arrival to the fertilization site and thus fertilize the ovum. The faster swimming speed in 2000-c1 case indicates that ND particles encourage hyperactivated swimming which negatively affects progressive movement. In addition, the ability of sperms to swim straighter also reduces sperm exhaustion nominating them for motility-based sperm selection [28].

Figure 4 shows the 3D AFM images of the witness and modified surfaces. The images prove the presence of ND particles on the surface but show insignificant change in roughness magnitude. The line-wise averages also do not show meaningful differences among the surfaces (495 nm for witness versus 501 nm for modified surface in average).
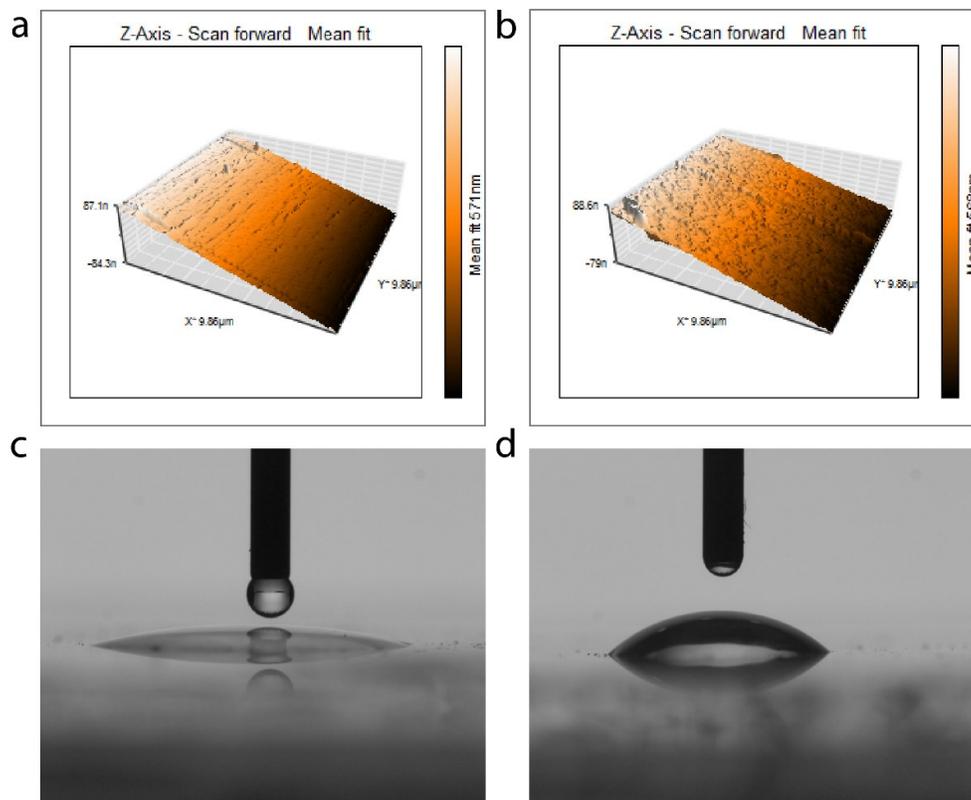

Fig. 4 Comparison between 3D surface profiles of the witness and ND-modified surfaces. (a) witness surface exhibits an average surface roughness of 571 nm, (b) The modified surface shows an average roughness of 568 nm in average. Surface roughness is showed to be almost unchanged but with the presence of ND particles on the surface. (c) Contact angle of the witness surface is 17.16° (d) Contact angle of the modified surface is 42.99° that shows 2.5-folds increase and indicates that the surface is made less hydrophilic.

Surprisingly, despite the insignificant change in surface roughness, the sperms exhibited improved behavior on the modified surfaces. Despite using several etching stages in this study, it is shown that the intentional roughening of the surface provided hosting sites for spin coated ND particles rather than the sperms. Thus, the reason behind such behavior would be the presence of ND particles on the surface. Similar sperm behavior was also reported by Sommer et al. which deposited Nano-diamond particles on IVF polystyrene petri dishes. They showed that grade A sperm's motion is enhanced by 300% [29]. The same authors showed that cells display improved climbing behavior on nanocrystalline diamond [30]. This behavior is supposed to be attributed with the rather ROS-free ND surfaces [29] that obviously calls for further investigation. From another standpoint, ND coating can reduce frictional coefficient of the surface by reducing the contact area of the sliding surface. It also significantly weakens the atomic drag force across the interface of two relatively moving surfaces

due to its inertness [31] which may be another explanation for such behavior. Moreover, based on Figures 4c and 4d, the modified surface shows increased contact angle magnitude compared to that of the witness by 2.5-folds. Still cannot be categorized as hydrophobic (contact angle>90 degrees), the modified surface shows decreased hydrophilicity. In this manner, the third explanation behind the improved behavior can be attributed to lessening of hydrophilicity.

4. Conclusion

The female reproductive tract is known to facilitate migration of sperms and micro/nanotechnologies offer the opportunity of mimicking the function of reproductive tract in vitro. Here we demonstrated that ND modified glass substrates improve the sperm motility from 5 to 85%. The results indicated that sperms swim straighter and with enhanced speed on the modified surfaces which in turn prevents sperm exhaustion. This behavior can root in rather ROS-free, friction-decreasing or less hydrophilic ND-modified surfaces.

This low-cost (4$ per unit area of modified surface) and combinational method with scale-up potential allows for extensive usage of ND modified surfaces in biological applications. Despite the time-consuming etching process, the method has high throughput where large numbers of glass substrates can be modified simultaneously. In particular, the present study would open new windows in front of the assisted reproductive techniques as IVF to modify their protocols and subsequently improve their outcomes. Moreover, the replacement of normal with modified glass in fertility-aid microfluidic devices can also enhance their efficiency and turn them into competitive rivals for traditional techniques along with preparing them for commercialization.

Author Contributions

A.L. and M.M.Z designed the research. A.L. performed research with assistance from H.M. for preparing the substrates and from S.K. for analyzing sperm concentration and conducting spectrophotometry experiments. A.L., I.R.S analyzed data. All authors were involved in writing and editing the paper.

Conflict of Interest

The authors declare no conflict of interests.

References

1. Zhang Z, L.J., Meriano J, Ru C, Xie S, Luo J, Sun Y, *Human sperm rheotaxis: a passive physical process.* Scientific Reports, 2016. **6**: p. 23553.
2. Rappa, K., et al., *Quantitative analysis of sperm rheotaxis using a microfluidic device.* Microfluidics and Nanofluidics, 2018. **22**(9): p. 100.
3. Vasily Kantsler, J.D., Martyn Blayney, Raymond E Goldstein, *Rheotaxis facilitates upstream navigation of mammalian sperm cells.* eLife, 2014. **3**: p. e02403.
4. Teves ME, G.H., Uñates DR, et al. , *Molecular mechanism for human sperm chemotaxis mediated by progesterone* PLoS One, 2009. **4**(12): p. e8211.
5. Yoshida, M. and K. Yoshida, *Sperm chemotaxis and regulation of flagellar movement by Ca2+.* MHR: Basic science of reproductive medicine, 2011. **17**(8): p. 457-465.
6. Ko YJ, M.J., Lee BC, Lee S, Hwang SY, Ahn Y, *Separation of progressive motile sperm from mouse semen using on-chip chemotaxis.* Anal Sci., 2012. **28**(1): p. 27-32.
7. Bahat A, T.-K.I., Gakamsky A, Giojalas LC, Breitbart H, Eisenbach M., *Thermotaxis of mammalian sperm cells: a potential navigation mechanism in the female genital tract.* Nature Medicine, 2003. **9**(2): p. 149-150.
8. Bahat A, E.M., *Sperm thermotaxis.* Mol Cell Endocrinol., 2006. **252**(1-2): p. 115-9.
9. Pérez-Cerezales S, L.-B.R., de Castro AC, et al. , *Sperm selection by thermotaxis improves ICSI outcome in mice.* Scientific Reports, 2018. **8**(1): p. 2902.
10. Smith, D.J.B., J. R., *Surface accumulation of spermatozoa: a fluid dynamic phenomenon.* Math. Sci., 2009. **34**: p. 74-87.
11. Woolley, D.M., *Motility of spermatozoa at surfaces.* Reproduction, 2003. **126**: p. 259-270.
12. Elgeti, J., Winkler, R. G. & Gompper, G. , *Physics of microswimmers - single particle motion and collective behavior: a review.* Rep. Prog. Phys., 2015. **78**: p. 56601.
13. Brumley, D.R., Wan, K. Y., Polin, M. & Goldstein, R. E. , *Flagellar synchronization through direct hydrodynamic interactions.* eLife, 2014. **3**: p. e02750.
14. Cosson, J., Huitorel, P. & Gagnon, C. , *How spermatozoa come to be confined to surfaces.* Cell. Motil. Cytoskeleton, 2003. **54**: p. 56-63.
15. Denissenko, P., Kantsler, V., Smith, D. J. & Kirkman- Brown, J. , *Human spermatozoa migration in microchannels reveals boundary-following navigation.* Proc. Natl Acad. Sci. USA, 2012. **109**: p. 8007-8010.
16. Dumitrascu, N., et al., *Roughness modification of surfaces treated by a pulsed dielectric barrier discharge.* Plasma Sources Science and Technology, 2002. **11**(2): p. 127-134.
17. Niu, Y., et al., *Understanding the contribution of surface roughness and hydrophobic modification of silica nanoparticles to enhanced therapeutic protein delivery.* Journal of Materials Chemistry B, 2016. **4**(2): p. 212-219.
18. Chen, C.H., et al., *Effect of surface modification on mechanical properties and thermal stability of Sm–Co high temperature magnetic materials.* Surface and Coatings Technology, 2006. **201**(6): p. 3430-3437.
19. Mills KL, Z.X., Takayama S, Thouless MD, *The mechanical properties of a surface-modified layer on poly(dimethylsiloxane).* J Mater Res. , 2008. **23**(1): p. 37-48.
20. Rupp, F., et al., *Enhancing surface free energy and hydrophilicity through chemical modification of microstructured titanium implant surfaces.* Journal of Biomedical Materials Research Part A, 2006. **76A**(2): p. 323-334.
21. Trantidou, T., et al., *Hydrophilic surface modification of PDMS for droplet microfluidics using a simple, quick, and robust method via PVA deposition.* Microsystems &Amp; Nanoengineering, 2017. **3**: p. 16091.
22. Alekhin, A.P., et al., *Synthesis of biocompatible surfaces by nanotechnology methods.* Nanotechnologies in Russia, 2010. **5**(9): p. 696-708.
23. Lin, P., et al., *Improving biocompatibility by surface modification techniques on implantable bioelectronics.* Biosensors and Bioelectronics, 2013. **47**: p. 451-460.

24. Vogler, E.A., *Surface Modification for Biocompatibility*, in *Engineered Biomimicry*. 2013, Elsevier Inc. p. 189-220.

25. Bertazzo, S. and K. Rezwan, *Control of α-Alumina Surface Charge with Carboxylic Acids.* Langmuir, 2010. **26**(5): p. 3364-3371.

26. López-Trosell, A. and R. Schomäcker, *Coating of glass surfaces with nanoparticles of different materials synthesized in microemulsions.* 2005 NSTI Nanotechnology Conference and Trade Show - NSTI Nanotech 2005 Technical Proceedings, 2005: p. 313-316.

27. Reza Nosrati, A.D., Christopher M. Yip & David Sinton, *Two-dimensional slither swimming of sperm within a micrometre of a surface.* Nature Communications, 2015. **6**: p. 8703.

28. Tasoglu, S.S., H. Zhang, X., Kingsley, J. L., Catalano, P. N., Gurkan, U. A., Nureddin, A., Kayaalp, E., Anchan, R. M., Maas, R. L., Tüzel, E., Demirci, U., *Exhaustion of racing sperm in nature-mimicking microfluidic channels during sorting.* Small, 2013. **9**(20): p. 3374-84.

29. Andrei P. Sommer, S.J., Maria R. Maduro, Katharina Hancke, Wolfgang Janni, Hans-Jörg Fecht, *Genesis on diamonds II: contact with diamond enhances human sperm performance by 300%.* Ann Transl Med, 2016. **4**(20): p. 407.

30. Andrei P. Sommer, D.Z., Friedrich Gagsteiger and Hans-Jörg Fecht, *Sperm Performance Better on Diamond than on Polystyrene.* Mater. Res. Soc. Symp. Proc., 2013. **15**.

31. Lin, J.C.S.a.J., *Diamond Nanotechnology Syntheses and Applications*. 2010: Pan Stanford Publishing Pte. Ltd.